

Distribution Aligning Refinery of Pseudo-label for Imbalanced Semi-supervised Learning

Jaehyung Kim¹, Youngbum Hur³, Sejun Park¹, Eunho Yang^{1,2}, Sung Ju Hwang^{1,2}, and
Jinwoo Shin¹

¹Korea Advanced Institute of Science and Technology (KAIST)

²AITRICS

³Samsung Advanced Institute of Technology

{jaehyungkim, sejun.park, sjhwang82, jinwoos}@kaist.ac.kr

{yangeh}@gmail.com

{youngbum.hur}@samsung.com

Abstract

While semi-supervised learning (SSL) has proven to be a promising way for leveraging unlabeled data when labeled data is scarce, the existing SSL algorithms typically assume that training class distributions are balanced. However, these SSL algorithms trained under imbalanced class distributions can severely suffer when generalizing to a balanced testing criterion, since they utilize biased pseudo-labels of unlabeled data toward majority classes. To alleviate this issue, we formulate a convex optimization problem to softly refine the pseudo-labels generated from the biased model, and develop a simple algorithm, named Distribution Aligning Refinery of Pseudo-label (DARP) that solves it provably and efficiently. Under various class-imbalanced semi-supervised scenarios, we demonstrate the effectiveness of DARP and its compatibility with state-of-the-art SSL schemes.

1 Introduction

It has been repeatedly shown that deep neural networks (DNNs) can achieve human- or super-human-level performances on various tasks [1, 18, 33]. This success, however, crucially relies on the availability of large-scale labeled datasets, which typically requires a lot of human efforts to be constructed. For example, the cost for labeling sequential (such as video and speech) data is often proportional to their lengths. Furthermore, some specific domain knowledge is often critical for labeling (such as medical) data. Semi-supervised learning (SSL) is one of the most promising ways to bypass this cost by leveraging unlabeled data for improving the performance of DNNs, given a small amount of labeled data [4, 5, 43]. The common approach of these modern state-of-the-art SSL algorithms is producing pseudo-labels for unlabeled data based on a model's prediction and then utilize the generated pseudo-labels for training the model iteratively [30, 38].

Most previous works on the line usually assume a balanced class distribution for labeled and unlabeled datasets. However, in many realistic scenarios, the underlying class distribution of training data is highly imbalanced [29, 39]. It is well known that such an imbalanced class distribution makes the generalization of DNNs poor and their predictions to be biased toward majority classes [14]. Hence, DNNs trained under an imbalanced class distribution suffer when generalizing to a balanced testing criterion. This issue can be more problematic for SSL algorithms since they generate pseudo-labels of unlabeled data from the model's biased predictions, i.e., pseudo-labels are even more severely imbalanced compared to true labels of labeled or unlabeled data. For example, when we train a Wide ResNet [44] on CIFAR-10 [13] under the imbalance

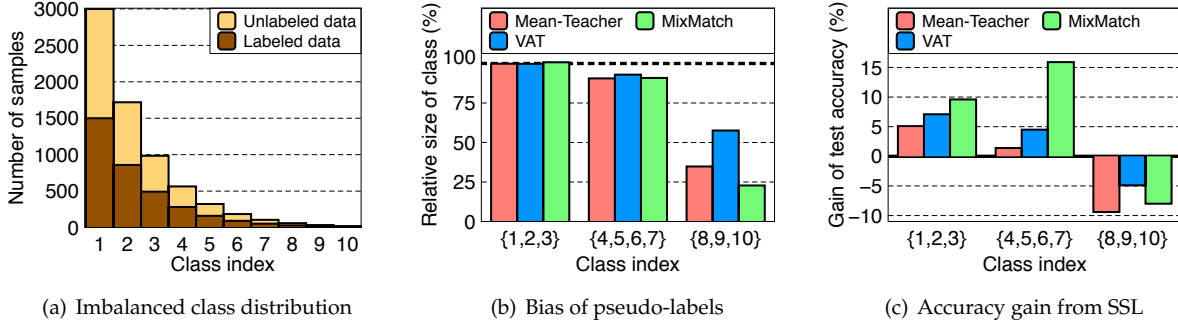


Figure 1: Experimental results on CIFAR-10 under the imbalance ratio $\gamma = 150$. (a) Class distribution of labeled and unlabeled data. (b) Relative size of pseudo-labels compares to size of true labels for each SSL algorithm. It is noticeable that the models fail to generate pseudo-labels on minority classes; hence the imbalance ratio of pseudo-labels is much larger than the true ratio. (c) Test accuracy gain due to SSL algorithms compares to the vanilla model trained using only labeled data.

ratio $\gamma = 150$ ¹ using a recent state-of-the-art SSL algorithm, MixMatch [5], the resulting imbalance ratio of pseudo-labels becomes $\gamma = 1046$, which is much larger than the true imbalance ratio $\gamma = 150$ (see Figure 1(b) for detailed class-wise statistics).

Due to the aforementioned reason, we found that the performance of classifiers trained by recent SSL algorithms under the imbalanced class distribution often degrades on minority classes, even compared to the vanilla scheme using only labeled training samples (see Figure 1(c)). This implies that utilizing imbalanced unlabeled data for training can be dangerous for the classes having relatively small number of samples. Identifying a potential risk under class-imbalanced SSL scenarios is an important but under-explored research problem.

Contribution. To alleviate the issue, we propose a simple technique, coined distribution aligning refinery of pseudo-label (DARP), applicable to any existing SSL scheme (as long as they utilize pseudo-labels of unlabeled data). Our high-level idea is to refine the original, biased pseudo-labels so that their distribution can match the true class distribution of unlabeled data. Importantly, we also constrain our refined pseudo-labels to be not too far from the original pseudo-labels (constructed by an SSL algorithm): otherwise, the individual quality of refined pseudo-labels can be poor, even when their overall distribution matches the true distribution. Motivated by the insight, we formulate an optimization problem for constructing refined pseudo-labels: minimizing the distortion from the original pseudo-labels, while matching the true class distribution.

The DARP algorithm is an efficient procedure to solve the proposed (convex) optimization with a provable guarantee; it finds the unique optimal solution by solving the Lagrangian dual of the original optimization with a simple iterative procedure. To further enhance the quality of the refined pseudo-labels, we additionally suggest removing some small and noisy entries in the original pseudo-labels when running DARP.

We demonstrate the effectiveness of the proposed approach under various realistic scenarios by varying the imbalanced class distributions. Despite its simplicity, the proposed DARP algorithm improves recent state-of-the-art SSL algorithms in all test cases, e.g., our method improves MixMatch [5], ReMixMatch [4] and FixMatch [37] with up to 77.2%, 31.4% and 53.1% relative reduction on the balanced test error, respectively. We find that our method is more effective when the (class) distribution mismatch between labeled and unlabeled data becomes severe. Such distribution mismatch has been under-explored in the literature on SSL but can occur under a realistic scenario.

¹The number of training samples of a class (in both labeled and unlabeled datasets is up to 150 times smaller than that of another class.

2 Related works

Learning with class-imbalanced data. Despite having several well-organized datasets in research, e.g., CIFAR [25] and ILSVRC [34], real-world datasets usually have a “long-tailed” label distribution [29, 39]. It is well-known that such *class-imbalanced* datasets make the standard training of DNN harder to generalize [14, 32, 40]. A natural approach to bypass this *class-imbalance problem* is re-balancing the training objective with respect to the class-wise sample sizes. Two of such methods are representative: (a) *re-weighting* the given loss function by a factor inversely proportional to the sample frequency in a class-wise manner [20, 23], and (b) *re-sampling* the given dataset so that the expected sampling distribution during training can be balanced [9, 17, 21]. However, naïvely re-balancing the objective usually results in harsh over-fitting to minority classes, so several attempts have been made to alleviate this issue: [13] proposed the concept of “effective number” for each class as alternative weights in the re-weighting method. [8, 22] found that both re-weighting and re-sampling can be much more effective when applied at the later stage of training, in case of DNNs. Recently, [28] suggested re-balancing the training objective using unlabeled data, but it performs much worse compared to recent state-of-the-art semi-supervised learning algorithms.

Semi-supervised learning. The goal of a semi-supervised learning (SSL) algorithm is to improve the model’s performance by leveraging unlabeled data to alleviate the need for labeled data. A popular class of SSL algorithms can be roughly viewed as producing a pseudo-label for each unlabeled data based on the model’s prediction and then training the model to predict the pseudo-label when the unlabeled data is given as input. For example, pseudo labeling [27] (also known as self-training [42, 43]) generates the pseudo-label using the model’s class prediction and trains the model with it again. Similarly, consistency regularization based methods obtain pseudo-label utilizing the model’s predicted distribution after arbitrarily modifying the input [30, 35] or model function [38]. Recent state-of-the-art SSL algorithms combine both schemes for producing better pseudo-labels [4, 5]. However, since the pseudo-label of the unlabeled data is generated from the model’s prediction, these methods can be inefficient or even harmful when the model’s prediction is biased toward majority classes due to the imbalanced class distribution (see Figure 1(c)).

3 Handling imbalanced semi-supervised learning

3.1 Pseudo-label under imbalanced semi-supervised learning

We first describe the problem setup of our interest. Consider a classification problem with K classes. Let $x \in \mathbb{R}^d$ and $y \in \{0, 1\}^K$ denote an input vector and corresponding one-hot label, respectively, where d is the dimension of the input. We assume the following datasets are available:

$$\mathcal{D}^{\text{labeled}} = \{(x_n^{\text{labeled}}, y_n^{\text{labeled}})\}_{n=1}^N, \quad \mathcal{D}^{\text{unlabeled}} = \{x_m^{\text{unlabeled}}\}_{m=1}^M,$$

where $\mathcal{D}^{\text{labeled}}, \mathcal{D}^{\text{unlabeled}}$ correspond to labeled and unlabeled datasets, respectively. Then, the goal of the learner is to train a classifier $f = [f_k]_{k=1}^K : \mathbb{R}^d \rightarrow [0, 1]^K$ using the above datasets: it outputs the predictive probability $f_k(x) \in [0, 1]$ for each class k given an input x . We also let $y_m^{\text{unlabeled}}$ denote the one-hot label of the true (yet unknown) class of $x_m^{\text{unlabeled}}$. The numbers of data in class k under $\mathcal{D}^{\text{labeled}}$ and $\mathcal{D}^{\text{unlabeled}}$ are denoted by N_k and M_k , respectively, i.e., $\sum_{k=1}^K N_k = N$ and $\sum_{k=1}^K M_k = M$. We are interested in class-imbalanced scenarios where $\frac{\max_k N_k}{\min_k N_k}$ and $\frac{\max_k M_k}{\min_k M_k}$ are much larger than 1 as illustrated in Figure 1(a).

To utilize the unlabeled training data effectively, most recent state-of-the-art SSL algorithms infer their labels by some pseudo-labels denoted by

$$\left\{ \hat{y}_m^{\text{unlabeled}} \in [0, 1]^K \mid \sum_{k=1}^K \hat{y}_m^{\text{unlabeled}}(k) = 1 \right\}_{m=1}^M.$$

Then, they train the model by optimizing supervised losses (e.g., cross-entropy) corresponding to $(x_n^{\text{labeled}},$

Algorithm 1 DualCoordinateAscent: Coordinate ascent algorithm for dual of (1)

Require: $\{\hat{y}_m^{\text{unlabeled}}\}_{m=1}^M$, $\{w_m\}_{m=1}^M$, $\{M_k\}_{k=1}^K$, T
Ensure: The unique solution of (1)

```

1:  $\hat{y}_m^0 \leftarrow \hat{y}_m^{\text{unlabeled}}$ ,  $X_m^0 \leftarrow 1$ ,  $Y_k^0 \leftarrow 1$ ,  $\forall m, k$ 
2: for  $t = 1$  to  $T$  do
3:   if  $t$  is odd or  $t = T$  then
4:      $X_m^t \leftarrow \left( \sum_{k=1}^K \hat{y}_m^0(k) (Y_k^{t-1})^{\frac{1}{w_m}} \right)^{-1}$ ,  $\forall m$ ,
5:      $Y_k^t \leftarrow Y_k^{t-1}$ ,  $\forall k$ 
6:   else
7:      $X_m^t \leftarrow X_m^{t-1}$ ,  $\forall m$ 
8:      $Y_k^t \leftarrow \text{Solve}_{Z \geq 0} \left( \sum_{m=1}^M \hat{y}_m^0(k) X_m^{t-1} Z^{\frac{1}{w_m}} - M_k \right)$ ,  $\forall k$ 2
9:   end if
10: end for
11:  $\hat{y}_m^{\text{out}}(k) \leftarrow \hat{y}_m^0(k) X_m^T (Y_k^T)^{\frac{1}{w_m}}$ ,  $\forall m, k$ 

```

$\hat{y}_n^{\text{labeled}}$) and $(x_m^{\text{unlabeled}}, \hat{y}_m^{\text{unlabeled}})$, possibly with other regularization losses, e.g., consistency loss [30, 38]. Hence, the performance of SSL algorithm is quite sensitive to the quality of pseudo-labels $\hat{y}_m^{\text{unlabeled}}$. However, the imbalanced class distribution incurs the bias of the model’s prediction toward majority classes of large N_k , and the resulting quality of the pseudo-labels can be significantly degraded. As reported in Figure 1(b), pseudo-labels can be more severely imbalanced than the truth. Hence, some SSL algorithms utilizing these pseudo-labels as direct supervision or a source of regularization can be ineffective or even harmful for minority classes (see Figure 1(c)).

3.2 Distribution aligning refinery of pseudo-label

Now, we present our technique, coined distribution aligning refinery of pseudo-label (DARP). The input of DARP could be any pseudo-labels constructed from any SSL algorithm, i.e., it can incorporate into various SSL algorithms for refining their outputs. In this section, we focus on describing how to refine pseudo-labels given the true class distribution of unlabeled data, i.e., $\{M_k\}_{k=1}^K$. As $\{M_k\}_{k=1}^K$ is not known for the learner in general, we will discuss how to estimate it in Section 4.2.

Refining pseudo-labels via optimization. Given the original pseudo-labels $\{\hat{y}_m^{\text{unlabeled}}\}_{m=1}^M$ (generated by an SSL algorithm), we are interested in refining them so that their class distribution matches the true distribution $\{M_k\}_{k=1}^K$. Simultaneously, we also want to preserve the original information in $\{\hat{y}_m^{\text{unlabeled}}\}_{m=1}^M$ as much as possible, to maintain the high quality of refined pseudo-labels. To this end, we propose the following convex optimization problem with respect to variables $\{\hat{y}_m\}_{m=1}^M$:

$$\begin{aligned}
 & \text{minimize} && \sum_{m=1}^M w_m D_{KL}(\hat{y}_m \parallel \hat{y}_m^{\text{unlabeled}}) \\
 & \text{subject to} && \sum_{m=1}^M \hat{y}_m(k) = M_k, \forall k, \sum_{k=1}^K \hat{y}_m(k) = 1, \forall m, \hat{y}_m(k) \in [0, 1], \forall m, k
 \end{aligned} \tag{1}$$

where the KL-divergence objective $D_{KL}(\hat{y}_m \parallel \hat{y}_m^{\text{unlabeled}})$ is to preserve the original information of $\hat{y}_m^{\text{unlabeled}}$ and the constraint $\sum_{m=1}^M \hat{y}_m(k) = M_k$ is to match to the true class distribution of unlabeled data. In particular, the above optimization is encouraged to preserve more information of high-confident original pseudo-labels by introducing weight w_m to each data by

$$w_m := (H(\hat{y}_m^{\text{unlabeled}}))^{-1},$$

² $\text{Solve}_{Z \geq 0}(f(Z))$ returns $Z \geq 0$ such that $f(Z) = 0$. We utilize the Newton’s method [15, 6] for $\text{Solve}_{Z \geq 0}(f(Z))$ in all experiments in this paper.

Algorithm 2 DARP: Distribution aligning refinery of pseudo-label

Input: unlabeled data $\{x_m^{\text{unlabeled}}\}_{m=1}^M$, pseudo-labels $\{\hat{y}_m^{\text{unlabeled}}\}_{m=1}^M$, sample-wise weights $\{w_m\}_{m=1}^M$, true class distribution $\{M_k\}_{k=1}^K$, number of classes K , number of iterations T , hyper-parameter for removing noisy pseudo-label entries α .

Output: Refined pseudo-labels \hat{y}_m^{DARP}

- 1: **for** $k = 1$ **to** K **do**
 - 2: $\{\hat{m}_1, \dots, \hat{m}_M\} \leftarrow \text{Sort}(\{y_m^{\text{unlabeled}}(k) \mid \forall m\})$
 - 3: $\mathcal{U}_k = \{x_{\hat{m}_1}^{\text{unlabeled}}, \dots, x_{\hat{m}_\alpha}^{\text{unlabeled}}\}, \hat{\alpha} = \lfloor \alpha \cdot M_k \rfloor$
 - 4: **end for**
 - 5: $\hat{y}_m^{\text{unlabeled}}(k) \leftarrow \begin{cases} \hat{y}_m^{\text{unlabeled}}(k) & \text{if } x_m^{\text{unlabeled}} \in \mathcal{U}_k \\ 0 & \text{otherwise} \end{cases}, X_m^0 = Y_k^0 = 1 \quad \forall m, k$
 - 6: $\hat{y}_m^{\text{DARP}}(k) \leftarrow \text{DualCoordinateAscent}(\{\hat{y}_m^{\text{unlabeled}}\}_{m=1}^M, \{w_m\}_{m=1}^M, \{M_k\}_{k=1}^K, T)$
-

i.e., larger weight to more confident data of smaller entropy H .

Solving the optimization (1), e.g., by some generic convex scheme, might incur much computational overhead, especially for refining a large number of pseudo-labels. To address this issue, we propose an efficient iterative procedure, Algorithm 1, for solving (1). In essence, it is a coordinate ascent algorithm for Lagrangian dual of (1), which alternatively finds the local optimum of each of dual variables $\{X_m\}_{m=1}^M$ and $\{Y_k\}_{k=1}^K$. We provide the following provable guarantee of Algorithm 1.

Theorem 1. *The output of Algorithm 1 converges to the unique solution of (1) as $T \rightarrow \infty$ unless $\sum_{m=1}^M w_m D_{\text{KL}}(\hat{y}_m \parallel \hat{y}_m^{\text{unlabeled}}) = \infty$ for all feasible $\{\hat{y}_m\}_{m=1}^M$.*

We present the proof of Theorem 1 in the supplementary material. We empirically observe that $T = 10$ is enough for the convergence in our experiments. Consequently, DARP increases at most 20% of the overall training time of an existing SSL scheme under our experimental setups.

Removing small entries of pseudo-labels. To further enhance the quality of pseudo-labels, we would concentrate on confident entries of the original pseudo-labels by removing small and noisy entries as below:

$$\hat{y}_m^0(k) \leftarrow \begin{cases} \hat{y}_m^{\text{unlabeled}}(k) & \text{if } x_m^{\text{unlabeled}} \in \mathcal{U}_k \\ 0 & \text{otherwise} \end{cases}, \quad (2)$$

where \mathcal{U}_k is the subset of top αM_k unlabeled data having larger values of $y_m^{\text{unlabeled}}(k)$ for some $\alpha > 0$. Namely, we clip the value of $y_m^{\text{unlabeled}}(k)$ to be zero if it is relatively small. At some angle, the initialization (2) is expected to decrease the entropy of \hat{y}_m^t , compared to the naïve initialization $\hat{y}_m^0 = \hat{y}_m^{\text{unlabeled}}$, which is similar to the entropy minimization technique used in the previous SSL algorithm [16] in spirit. The full details of the proposed DARP are described in Algorithm 2.

4 Experiments

In this section, we evaluate our algorithm on various scenarios for imbalanced semi-supervised learning in classification problems.³ We first describe the experimental setups in Section 4.1. In Section 4.2, we present empirical evaluations on DARP and other baseline algorithms under various setups. In Section 4.3, we present detailed analysis on DARP.

³Code is available at <https://github.com/bbuing9/DARP>

4.1 Experimental setup

Imbalanced dataset. We primarily consider a “synthetically long-tailed” variant of CIFAR-10 in order to evaluate our algorithm under various levels of imbalance. Results for other datasets are given in the supplementary material. For constructing the class-imbalanced training dataset, without loss of generality, we assume the ordered numbers of labeled data in each class as $N_1 \geq \dots \geq N_K$. We use a single parameter $\gamma_l \geq 1$, called the *imbalance ratio*, to control the class-imbalance of the labeled dataset: once γ_l and N_1 are given, we set $N_k = N_1 \cdot \gamma_l^{-\frac{k-1}{K-1}}$ so that $N_1 = \gamma_l \cdot N_K$ as done by [13]. Namely, larger γ_l indicates more class-imbalanced distribution. Likewise, we assume that $M_1 \geq \dots \geq M_K$ for the unlabeled dataset and its imbalance is controlled by $\gamma_u \geq 1$, as we did for the labeled dataset. We use $N_1 = 1500, M_1 = 3000$ as the default values. Figure 1(a) illustrates the constructed imbalanced class distribution on CIFAR-10 with $\gamma_l = \gamma_u = 150$. To evaluate the classification performance of models trained under the imbalanced dataset, we report two popular metrics: *balanced accuracy* (bACC) [20, 40] and *geometric mean scores* (GM) [7, 26], which are defined by the arithmetic and geometric mean over class-wise sensitivity, respectively. In this section, mean and standard deviation are reported across three random trials, respectively.

Baselines. We compare our algorithm with various baselines, including recent re-balancing algorithms for learning with class-imbalanced labeled data only (i.e., without using unlabeled data) and semi-supervised learning algorithms for learning with both labeled and unlabeled data (i.e., without considering class-imbalance). We first consider a naïve baseline without any re-balancing and using unlabeled data, denoted by (a) Vanilla. Then, we consider a wide range of previous “re-balancing” algorithms denoted by (b) Re-sampling [21]: each class is equally sampled for training; (c) Label-distribution-aware margin (LDAM-DRW) [8]: the classifier is trained to impose larger margin to minority classes and balancing the objective at the later stage of training; (d) Classifier re-training (cRT) [22]: only re-train the classifier with the balanced objective after training a whole network under imbalanced distribution. We also consider a wide range of previous “semi-supervised learning” algorithms denoted by (e) Virtual adversarial training (VAT) [30]: for unlabeled data, consistency regularization with its adversarial example is added; (f) Mean-Teacher [38]: adding consistency regularization between the prediction of the current model and the ensemble of previous models; (g) MixMatch [5]: both pseudo-label and consistency regularization are applied with Mixup regularization [45]; (h) ReMixMatch [4]: MixMatch is further improved with an augmentation anchoring and a distribution alignment. (i) FixMatch [37]: strongly augmented unlabeled data are used for training where their pseudo-labels are generated from their weakly augmented version. Details on the implementation of the baseline algorithms are presented in the supplementary material.

Training details. All experiments are conducted with Wide ResNet-28-2 [31] and it is trained with batch size 64 for 2.5×10^5 training iterations. For all algorithms, we evaluate the model on the test dataset for every 500 iterations and report the average test accuracy of the last 20 evaluations following [5]. We apply the DARP procedure for every 10 iterations with fixed hyper-parameters $\alpha = 2$ and $T = 10$, which is empirically enough for the convergence of DARP. Since pseudo-labels are not accurate at the early stage of training, we are not using DARP until the first 40% of iterations. More training details are presented in the supplementary material.

4.2 Imbalanced semi-supervised learning

We evaluate DARP with both re-balancing (RB) and semi-supervised learning (SSL) algorithms under various levels of class-imbalance. In particular, we study two cases $\gamma_u = \gamma_l$ and $\gamma_u \neq \gamma_l$. We apply DARP to recent state-of-the-art SSL algorithms: MixMatch [5], ReMixMatch [4] and FixMatch [37], denoted by MixMatch+DARP, ReMixMatch+DARP and FixMatch+DARP, respectively, and observe the gain due to DARP.

Case of $\gamma_l = \gamma_u$. We first conduct experiments in the case $\gamma := \gamma_l = \gamma_u$. This is arguably the most natural scenario that each data in both datasets is sampled from the same distribution. Here, we choose $M_k \propto N_k$ for both DARP and ReMixMatch. To verify the effectiveness of DARP in this scenario, we compare DARP with various semi-supervised learning (SSL) algorithms and re-balancing (RB) algorithms on CIFAR-10 with

Table 1: Comparison of classification performance (bACC/GM) on CIFAR-10 under three different class-imbalance ratio $\gamma = \gamma_l = \gamma_u$. SSL denotes semi-supervised learning and RB denotes re-balancing. The numbers in brackets below the gray rows are relative test error gains from DARP, compared to applied baseline SSL algorithms, respectively. The best results are indicated in bold.

Algorithm			CIFAR-10		
	SSL	RB	$\gamma = 50$	$\gamma = 100$	$\gamma = 150$
Vanilla	-	-	65.2 \pm 0.05 / 61.1 \pm 0.09	58.8 \pm 0.13 / 51.0 \pm 0.11	55.6 \pm 0.43 / 44.0 \pm 0.98
Re-sampling [21]	-	✓	64.3 \pm 0.48 / 60.6 \pm 0.67	55.8 \pm 0.47 / 45.1 \pm 0.30	52.2 \pm 0.05 / 38.2 \pm 1.49
LDAM-DRW [8]	-	✓	68.9 \pm 0.07 / 67.0 \pm 0.08	62.8 \pm 0.17 / 58.9 \pm 0.60	57.9 \pm 0.20 / 50.4 \pm 0.30
cRT [22]	-	✓	67.8 \pm 0.13 / 66.3 \pm 0.15	63.2 \pm 0.45 / 59.9 \pm 0.40	59.3 \pm 0.10 / 54.6 \pm 0.72
VAT [30]	✓	-	70.6 \pm 0.29 / 67.8 \pm 0.19	62.6 \pm 0.40 / 55.1 \pm 0.56	57.9 \pm 0.42 / 46.3 \pm 0.47
Mean-Teacher [38]	✓	-	68.8 \pm 1.05 / 64.9 \pm 1.53	60.9 \pm 0.33 / 52.8 \pm 0.81	54.5 \pm 0.22 / 39.8 \pm 0.73
MixMatch [5]	✓	-	73.2 \pm 0.56 / 68.9 \pm 1.15	64.8 \pm 0.28 / 49.0 \pm 2.05	62.5 \pm 0.31 / 42.5 \pm 1.68
MixMatch + DARP	✓	-	75.2 \pm 0.47 / 72.8 \pm 0.63 (-7.41% / -12.6%)	67.9 \pm 0.14 / 61.2 \pm 0.15 (-8.77% / -23.8%)	65.8 \pm 0.52 / 56.5 \pm 2.08 (-8.69% / -24.4%)
ReMixMatch [4]	✓	-	81.5 \pm 0.26 / 80.2 \pm 0.32	73.8 \pm 0.38 / 69.5 \pm 0.84	69.9 \pm 0.47 / 62.5 \pm 0.35
ReMixMatch + DARP	✓	-	82.1 \pm 0.14 / 80.8 \pm 0.09 (-3.45% / -3.52%)	75.8 \pm 0.09 / 72.6 \pm 0.24 (-7.84% / -10.2%)	71.0 \pm 0.27 / 64.5 \pm 0.68 (-3.60% / -5.19%)
FixMatch [37]	✓	-	79.2 \pm 0.33 / 77.8 \pm 0.36	71.5 \pm 0.72 / 66.8 \pm 1.51	68.4 \pm 0.15 / 59.9 \pm 0.43
FixMatch + DARP	✓	-	81.8 \pm 0.24 / 80.9 \pm 0.28 (-12.9% / -14.1%)	75.5 \pm 0.05 / 73.0 \pm 0.09 (-14.0% / -18.8%)	70.4 \pm 0.25 / 64.9 \pm 0.17 (-22.4% / -20.3%)

various γ . Table 1 summarizes the performance of baseline algorithms with/without DARP for learning CIFAR-10. It is noticeable that many SSL algorithms perform worse than RB algorithms, even they use more training (unlabeled) data. We observe that this is because the pseudo-labels of SSL algorithms generated from the biased models are likely to follow the majority classes of labeled data (see Figure 2(a)). Hence, utilizing these biased pseudo-labels for training can be ineffective or even harmful. On the other hand, DARP refines such biased pseudo-labels correctly (see Figure 2(c)), and consequently, it improves the performance of all the applied SSL algorithms: MixMatch, ReMixMatch and FixMatch. For example, DARP exhibits 22.4%/20.3% relative error gain of bACC/GM in the case of FixMatch under $\gamma = 150$. While DARP outperforms all the baselines, it could be further improved by combining with RB algorithms. Due to the space constraint, we present the results of DARP+cRT in the supplementary material.

Case of $\gamma_l \neq \gamma_u$. In contrast, the imbalance ratio of unlabeled data may not be the same as that of labeled data in general, i.e., $\gamma_l \neq \gamma_u$ and γ_u is unknown. Namely, we need to estimate $\{M_k\}_{k=1}^K$ for both ReMixMatch and DARP. Hence, we estimate it based on the linear relationship derived from the definition of a confusion matrix $C^{\text{unlabeled}} \in \mathbb{R}^{K \times K}$:

$$\begin{bmatrix} M_1 \\ \vdots \\ M_K \end{bmatrix} = (C^{\text{unlabeled}})^{-1} \times \begin{bmatrix} \sum_{m=1}^M f_1(x_m^{\text{unlabeled}}) \\ \vdots \\ \sum_{m=1}^M f_K(x_m^{\text{unlabeled}}) \end{bmatrix}, C_{ij}^{\text{unlabeled}} := \frac{\sum_{m: y_m^{\text{unlabeled}}(j)=1} f_i(x_m^{\text{unlabeled}})}{|\{m \mid y_m^{\text{unlabeled}}(j) = 1\}|}$$

where $C_{ij}^{\text{unlabeled}}$ denote the empirical probability that the model predicts class i when the true class is j . Since $y_n^{\text{unlabeled}}$ is not available, we approximate $C^{\text{unlabeled}}$ using some small subset of the labeled dataset, which is not used for the training until the confusion matrix is estimated. Here, we note that algorithms not requiring $\{M_k\}_{k=1}^K$ fully utilize the labeled dataset at training. Likewise, algorithms requiring $\{M_k\}_{k=1}^K$ utilize this small subset for their training procedure after estimating $C^{\text{unlabeled}}$. More details about this can be found in the supplementary material.

Table 2 summarizes the experimental results under $\gamma_l \neq \gamma_u$. Here, we denote ‘‘ReMixMatch’’ for ReMixMatch without estimation of $\{M_k\}_{k=1}^K$, i.e., it assumes $M_k \propto N_k$, and ‘‘ReMixMatch*’’ for ReMixMatch with

Table 2: Comparison of classification performance (bACC/GM) on CIFAR-10 under four different class-imbalance ratio γ_u with $\gamma_l = 100$. SSL denotes semi-supervised learning and RB denotes re-balancing. The numbers in brackets below the gray rows are relative test error gains from DARP, compared to applied baseline SSL algorithms, respectively. The best results are indicated in bold.

CIFAR-10 ($\gamma_l = 100$)							
Algorithm	SSL	RB	$\gamma_u = 1$	$\gamma_u = 50$	$\gamma_u = 150$	$\gamma_u = 100$ (reversed)	
Vanilla	-	-	58.8 \pm 0.13 / 51.0 \pm 0.11	58.8 \pm 0.13 / 51.0 \pm 0.11	58.8 \pm 0.13 / 51.0 \pm 0.11	58.8 \pm 0.13 / 51.0 \pm 0.11	
Re-sampling [21]	-	✓	55.8 \pm 0.47 / 45.1 \pm 0.30	55.8 \pm 0.47 / 45.1 \pm 0.30	55.8 \pm 0.47 / 45.1 \pm 0.30	55.8 \pm 0.47 / 45.1 \pm 0.30	
LDAM-DRW [8]	-	✓	62.8 \pm 0.17 / 58.9 \pm 0.60	62.8 \pm 0.17 / 58.9 \pm 0.60	62.8 \pm 0.17 / 58.9 \pm 0.60	62.8 \pm 0.17 / 58.9 \pm 0.60	
cRT [22]	-	✓	63.2 \pm 0.45 / 59.9 \pm 0.40	63.2 \pm 0.45 / 59.9 \pm 0.40	63.2 \pm 0.45 / 59.9 \pm 0.40	63.2 \pm 0.45 / 59.9 \pm 0.40	
VAT [30]	✓	-	65.2 \pm 0.12 / 59.5 \pm 0.26	64.0 \pm 0.31 / 57.3 \pm 0.66	62.8 \pm 0.19 / 55.1 \pm 0.70	59.4 \pm 0.36 / 50.6 \pm 0.61	
Mean-Teacher [38]	✓	-	73.9 \pm 1.19 / 71.7 \pm 1.42	61.2 \pm 0.51 / 53.5 \pm 0.84	59.7 \pm 0.50 / 50.0 \pm 1.61	61.0 \pm 0.82 / 56.4 \pm 1.64	
MixMatch [5]	✓	-	41.5 \pm 0.76 / 12.0 \pm 1.34	64.1 \pm 0.58 / 48.3 \pm 0.70	65.5 \pm 0.64 / 51.1 \pm 2.41	47.9 \pm 0.09 / 20.5 \pm 0.85	
MixMatch + DARP	✓	-	86.7 \pm 0.80 / 86.2 \pm 0.82	68.3 \pm 0.47 / 62.2 \pm 1.21	66.7 \pm 0.25 / 58.8 \pm 0.42	72.9 \pm 0.24 / 71.0 \pm 0.32	
			(-77.2% / -84.4%)	(-11.8% / -27.0%)	(-3.62% / -15.7%)	(-48.0% / -63.6%)	
ReMixMatch [4]	✓	-	48.3 \pm 0.14 / 19.5 \pm 0.85	75.1 \pm 0.43 / 71.9 \pm 0.77	72.5 \pm 0.10 / 68.2 \pm 0.32	49.0 \pm 0.55 / 17.1 \pm 1.48	
ReMixMatch*	✓	-	85.0 \pm 1.35 / 84.3 \pm 1.55	77.0 \pm 0.12 / 74.7 \pm 0.04	72.8 \pm 0.10 / 68.8 \pm 0.21	75.3 \pm 0.03 / 72.3 \pm 0.04	
ReMixMatch* + DARP	✓	-	89.7 \pm 0.15 / 89.4 \pm 0.17	77.4 \pm 0.22 / 75.0 \pm 0.25	73.2 \pm 0.11 / 69.2 \pm 0.31	80.1 \pm 0.11 / 78.5 \pm 0.17	
			(-31.4% / -32.5%)	(-1.72% / -1.49%)	(-1.53% / -2.64%)	(-19.5% / -22.5%)	
FixMatch [37]	✓	-	68.9 \pm 1.95 / 42.8 \pm 8.11	73.9 \pm 0.25 / 70.5 \pm 0.52	69.6 \pm 0.60 / 62.6 \pm 1.11	65.5 \pm 0.05 / 26.0 \pm 0.44	
FixMatch + DARP	✓	-	85.4 \pm 0.55 / 85.0 \pm 0.65	77.3 \pm 0.17 / 75.5 \pm 0.21	72.9 \pm 0.24 / 69.5 \pm 0.18	74.9 \pm 0.51 / 72.3 \pm 1.13	
			(-53.1% / -73.8%)	(-13.3% / -17.0%)	(-10.9% / -18.4%)	(-31.3% / -60.3%)	

Table 3: Comparison of classification performance (bACC/GM) on CIFAR-10 across different distribution matching methods applied to ReMixMatch [4] under $\gamma_l = 100$.

Algorithm	$\gamma_u = 1$	$\gamma_u = 50$	$\gamma_u = 100$	$\gamma_u = 100$ (reversed)
[2]	81.4 / 80.5	76.0 / 72.7	72.5 / 67.8	72.9 / 67.1
[4]	85.0 / 84.3	77.0 / 74.7	73.8 / 69.5	75.3 / 72.3
DARP	89.7 / 89.4	77.4 / 75.0	75.8 / 72.6	80.1 / 78.5

estimation of $\{M_k\}_{k=1}^K$. In Table 2, one can observe that DARP consistently improves all the baselines. Surprisingly, the relative error gain from DARP increases as γ_u decreases, i.e., the overall class-distribution becomes more balanced. We believe that this is because SSL algorithms without DARP cannot fully enjoy this more balanced distribution as their pseudo-labels of minority class data are significantly biased toward majority classes. Meanwhile, DARP correctly refines pseudo-labels to (approximately) follow the true class-distribution, and hence it can take advantage of a more balanced class distribution of unlabeled dataset.

To further investigate this phenomenon, we also evaluate algorithms for unlabeled dataset with reversely ordered class-distribution, i.e., $M_1 \leq \dots \leq M_K$ and $M_k = M_1 \cdot \gamma_u^{-\frac{k-1}{K-1}}$ for $\gamma_u = 100$, denoted by “ $\gamma_u = 100$ (reversed)” in Table 2. As expected, SSL algorithms fail as they provide wrong pseudo-labels to the most of unlabeled data (which are majority in unlabeled data while minority in labeled data). In contrast, DARP successfully refines these pseudo-labels and significantly improves baselines as in prior experiments. For example, DARP exhibits 19.5%/22.5% relative error gains of bACC/GM compared to the second-best method ReMixMatch* under $\gamma_u = 100$ (reversed).

4.3 Detailed analysis on DARP

Comparison with other distribution matching. The main motivation of DARP is to correct bias in pseudo-labels by matching the class distribution of pseudo-labels and true class distribution of unlabeled data. In

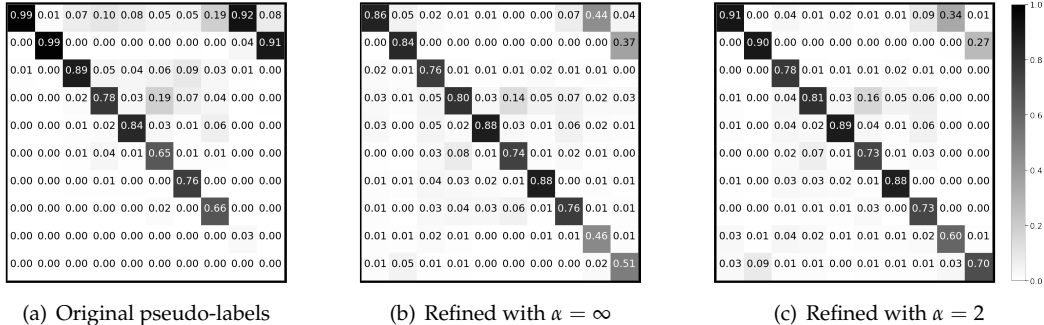


Figure 2: Confusion matrices of pseudo-labels on CIFAR-10 under $\gamma_l = 100, \gamma_u = 1$ using MixMatch [5]. (a) is from the original pseudo-labels. (b) and (c) are from refined pseudo-labels via DARP under $\alpha = \infty$ and $\alpha = 2$, i.e., without/with removing small entries, respectively.

this aspect, we compare DARP with the other distribution matching algorithms [2, 4], which are originally proposed under the balanced labeled/unlabeled class distributions, but applicable to any imbalanced settings. [2] directly adds the KL divergence loss as a regularizer where the class distribution of pseudo-labels is approximated within a mini-batch for optimizing loss. [4] proposes the “distribution alignment” procedure, which re-scales pseudo-labels to match the class distribution and then re-normalize them to satisfy the probability constraint. However, both methods cannot guarantee the exact distribution matching. Table 3 clearly shows that DARP provides larger performance gains compared to other algorithms. Note that we use the same target distribution $\{M_k\}_{k=1}^K$ for all algorithms. Here, one can observe that the performance gap between DARP and other algorithms becomes significant as the mismatch of labeled and unlabeled datasets becomes severe. This is because DARP exactly matches the distributions, while other algorithms do not.

Quality of refined pseudo-labels. We further evaluate DARP by measuring the error from refined pseudo-labels using underlying true labels hidden to DARP. For this, we use the model trained on CIFAR-10 under $\gamma_l = 100, \gamma_u = 1$ using MixMatch [5], which originally suffers from the biased pseudo-labels (see Figure 1(b)). Figure 2 visualizes the confusion matrix $C^{\text{unlabeled}}$ of pseudo-labels and refined pseudo-labels where $C^{\text{unlabeled}}$ is defined in Section 4.2. As expected, the original pseudo-labels are highly biased toward majority classes of the labeled dataset, i.e., small class indices. On the other hand, refined pseudo-labels are more likely to be unbiased compared to the original one, and the quality of pseudo-labels is significantly improved, especially in minority classes. In particular, for small α , the confusion matrix is less biased, while it is more biased for large α . We explain such an observation as follows: given α , the number of possible k -th nonzero entries in all refined pseudo-labels is restricted by αM_k . Here, large α allows more freedom in the choice of entries of the refined pseudo-labels, which would result in a smaller distortion from the original biased pseudo-labels (see our optimization objective (1)). Hence, for large α , the resulting refined pseudo-labels are likely to preserve the original pseudo-labels’ properties, including its bias. Besides, small α regularizes the entries of refined pseudo-labels and hence, reduces the bias of the original pseudo-labels. The effect of other components of DARP is presented in the supplementary material.

5 Conclusion

In this paper, we propose a simple and effective method to refine pseudo-labels for semi-supervised learning (SSL) under assuming class-imbalanced training distributions. Our main idea is to refine the biased pseudo-labels (generated by an SSL algorithm) so that (a) their distribution match to the true class distribution and (b) they still preserve the information of the original pseudo-label as much as possible. To further increase the quality of the refined pseudo-labels, we suggest to remove some noisy entries in the original pseudo-labels. Our method is quite easy-to-use to be adapted to any SSL algorithms. The class-imbalanced SSL scenarios are under-explored in the literature, and we think our work can be a strong guideline when other researchers pursue these tasks in the future.

Acknowledgements

This work was supported by Samsung Electronics and Institute of Information & communications Technology Planning & Evaluation (IITP) grant funded by the Korea government (MSIT) (No.2019-0-00075, Artificial Intelligence Graduate School Program (KAIST)).

References

- [1] Dario Amodei, Sundaram Ananthanarayanan, Rishita Anubhai, Jingliang Bai, Eric Battenberg, Carl Case, Jared Casper, Bryan Catanzaro, Qiang Cheng, Guoliang Chen, et al. Deep speech 2: End-to-end speech recognition in english and mandarin. In *Proceedings of the International Conference on Machine Learning (ICML)*, 2016.
- [2] Eric Arazo, Diego Ortego, Paul Albert, Noel E O'Connor, and Kevin McGuinness. Pseudo-labeling and confirmation bias in deep semi-supervised learning. *arXiv preprint arXiv:1908.02983*, 2019.
- [3] Kamyar Azizzadenesheli, Anqi Liu, Fanny Yang, and Animashree Anandkumar. Regularized learning for domain adaptation under label shifts. In *International Conference on Learning Representations (ICLR)*, 2019.
- [4] David Berthelot, Nicholas Carlini, Ekin D Cubuk, Alex Kurakin, Kihyuk Sohn, Han Zhang, and Colin Raffel. Remixmatch: Semi-supervised learning with distribution alignment and augmentation anchoring. In *International Conference on Learning Representations (ICLR)*, 2020.
- [5] David Berthelot, Nicholas Carlini, Ian Goodfellow, Nicolas Papernot, Avital Oliver, and Colin A Raffel. Mixmatch: A holistic approach to semi-supervised learning. In *Advances in Neural Information Processing Systems (NeurIPS)*, 2019.
- [6] Stephen Boyd and Lieven Vandenberghe. *Convex optimization*. Cambridge university press, 2004.
- [7] Paula Branco, Luís Torgo, and Rita P Ribeiro. A survey of predictive modeling on imbalanced domains. *ACM Computing Surveys (CSUR)*, 49(2):31, 2016.
- [8] Kaidi Cao, Colin Wei, Adrien Gaidon, Nikos Arechiga, and Tengyu Ma. Learning imbalanced datasets with label-distribution-aware margin loss. In *Advances in Neural Information Processing Systems (NeurIPS)*, 2019.
- [9] Nitesh V Chawla, Kevin W Bowyer, Lawrence O Hall, and W Philip Kegelmeyer. SMOTE: synthetic minority over-sampling technique. *Journal of Artificial Intelligence Research*, 2002.
- [10] Adam Coates, Andrew Ng, and Honglak Lee. An analysis of single-layer networks in unsupervised feature learning. In *Proceedings of the fourteenth international conference on artificial intelligence and statistics (AISTATS)*, 2011.
- [11] Imre Csiszár. I-divergence geometry of probability distributions and minimization problems. *The annals of probability*, pages 146–158, 1975.
- [12] Ekin D Cubuk, Barret Zoph, Jonathon Shlens, and Quoc V Le. Randaugment: Practical automated data augmentation with a reduced search space. *arXiv preprint arXiv:1909.13719*, 2019.
- [13] Yin Cui, Menglin Jia, Tsung-Yi Lin, Yang Song, and Serge Belongie. Class-balanced loss based on effective number of samples. In *Proceedings of the IEEE Conference on Computer Vision and Pattern Recognition (CVPR)*, 2019.
- [14] Qi Dong, Shaogang Gong, and Xiatian Zhu. Imbalanced deep learning by minority class incremental rectification. *IEEE Transactions on Pattern Analysis and Machine Intelligence*, 2018.

- [15] Aurel Galántai. The theory of newton’s method. *Journal of Computational and Applied Mathematics*, 124(1-2):25–44, 2000.
- [16] Yves Grandvalet and Yoshua Bengio. Semi-supervised learning by entropy minimization. In *Advances in Neural Information Processing Systems (NeurIPS)*, 2005.
- [17] Haibo He and Edwardo A Garcia. Learning from imbalanced data. *IEEE Transactions on Knowledge and Data Engineering (TKDE)*, 2008.
- [18] Kaiming He, Xiangyu Zhang, Shaoqing Ren, and Jian Sun. Deep residual learning for image recognition. In *Proceedings of the IEEE Conference on Computer Vision and Pattern Recognition (CVPR)*, 2016.
- [19] Dan Hendrycks, Mantas Mazeika, Duncan Wilson, and Kevin Gimpel. Using trusted data to train deep networks on labels corrupted by severe noise. In *Advances in Neural Information Processing Systems (NeurIPS)*, pages 10456–10465, 2018.
- [20] Chen Huang, Yining Li, Chen Change Loy, and Xiaoou Tang. Learning deep representation for imbalanced classification. In *Proceedings of the IEEE Conference on Computer Vision and Pattern Recognition (CVPR)*, 2016.
- [21] Nathalie Japkowicz. The class imbalance problem: Significance and strategies. In *Proceedings of the International Conference on Artificial Intelligence (ICAI)*, 2000.
- [22] Bingyi Kang, Saining Xie, Marcus Rohrbach, Zhicheng Yan, Albert Gordo, Jiashi Feng, and Yannis Kalantidis. Decoupling representation and classifier for long-tailed recognition. In *International Conference on Learning Representations (ICLR)*, 2020.
- [23] Salman H Khan, Munawar Hayat, Mohammed Bennamoun, Ferdous A Sohel, and Roberto Togneri. Cost-sensitive learning of deep feature representations from imbalanced data. *IEEE Transactions on Neural Networks and Learning Systems (TNNLS)*, 2017.
- [24] Diederik P Kingma and Jimmy Ba. Adam: A method for stochastic optimization. *International Conference on Learning Representations (ICLR)*, 2015.
- [25] Alex Krizhevsky. Learning multiple layers of features from tiny images. Technical report, Department of Computer Science, University of Toronto, 2009.
- [26] M Kubat. Addressing the curse of imbalanced training sets: One-sided selection. In *Proceedings of the International Conference on Machine Learning (ICML)*, pages 179–186, 1997.
- [27] Dong-Hyun Lee. Pseudo-label: The simple and efficient semi-supervised learning method for deep neural networks. In *Workshop on challenges in representation learning (ICML)*, 2013.
- [28] Yunru Liu, Tingran Gao, and Haizhao Yang. Selectnet: Learning to sample from the wild for imbalanced data training. *arXiv preprint arXiv:1905.09872*, 2019.
- [29] Dhruv Mahajan, Ross Girshick, Vignesh Ramanathan, Kaiming He, Manohar Paluri, Yixuan Li, Ashwin Bharambe, and Laurens van der Maaten. Exploring the limits of weakly supervised pretraining. In *Proceedings of the European Conference on Computer Vision (ECCV)*, 2018.
- [30] Takeru Miyato, Shin-ichi Maeda, Masanori Koyama, and Shin Ishii. Virtual adversarial training: a regularization method for supervised and semi-supervised learning. *IEEE Transactions on Pattern Analysis and Machine Intelligence*, 2018.
- [31] Avital Oliver, Augustus Odena, Colin A Raffel, Ekin Dogus Cubuk, and Ian Goodfellow. Realistic evaluation of deep semi-supervised learning algorithms. In *Advances in Neural Information Processing Systems (NeurIPS)*, pages 3235–3246, 2018.
- [32] Mengye Ren, Wenyan Zeng, Bin Yang, and Raquel Urtasun. Learning to reweight examples for robust deep learning. In *Proceedings of the International Conference on Machine Learning (ICML)*, 2018.

- [33] Shaoqing Ren, Kaiming He, Ross Girshick, and Jian Sun. Faster r-cnn: Towards real-time object detection with region proposal networks. In *Advances in Neural Information Processing Systems (NeurIPS)*, 2015.
- [34] Olga Russakovsky, Jia Deng, Hao Su, Jonathan Krause, Sanjeev Satheesh, Sean Ma, Zhiheng Huang, Andrej Karpathy, Aditya Khosla, Michael Bernstein, Alexander C. Berg, and Li Fei-Fei. ImageNet Large Scale Visual Recognition Challenge. *International Journal of Computer Vision (IJCV)*, 115(3):211–252, 2015.
- [35] Mehdi Sajjadi, Mehran Javanmardi, and Tolga Tasdizen. Regularization with stochastic transformations and perturbations for deep semi-supervised learning. In *Advances in Neural Information Processing Systems (NeurIPS)*, 2016.
- [36] Morton Slater. Lagrange multipliers revisited. In *Traces and Emergence of Nonlinear Programming*, pages 293–306. Springer, 2014.
- [37] Kihyuk Sohn, David Berthelot, Chun-Liang Li, Zizhao Zhang, Nicholas Carlini, Ekin D Cubuk, Alex Kurakin, Han Zhang, and Colin Raffel. Fixmatch: Simplifying semi-supervised learning with consistency and confidence. *arXiv preprint arXiv:2001.07685*, 2020.
- [38] Antti Tarvainen and Harri Valpola. Mean teachers are better role models: Weight-averaged consistency targets improve semi-supervised deep learning results. In *Advances in Neural Information Processing Systems (NeurIPS)*, 2017.
- [39] Grant Van Horn, Oisin Mac Aodha, Yang Song, Yin Cui, Chen Sun, Alex Shepard, Hartwig Adam, Pietro Perona, and Serge Belongie. The inaturalist species classification and detection dataset. In *Proceedings of the IEEE Conference on Computer Vision and Pattern Recognition (CVPR)*, 2018.
- [40] Yu-Xiong Wang, Deva Ramanan, and Martial Hebert. Learning to model the tail. In *Advances in Neural Information Processing Systems (NeurIPS)*, 2017.
- [41] Jianxiong Xiao, James Hays, Krista A Ehinger, Aude Oliva, and Antonio Torralba. Sun database: Large-scale scene recognition from abbey to zoo. In *Proceedings of the IEEE Conference on Computer Vision and Pattern Recognition (CVPR)*, pages 3485–3492. IEEE, 2010.
- [42] Qizhe Xie, Zihang Dai, Eduard Hovy, Minh-Thang Luong, and Quoc V Le. Unsupervised data augmentation. *arXiv preprint arXiv:1904.12848*, 2019.
- [43] Qizhe Xie, Eduard Hovy, Minh-Thang Luong, and Quoc V Le. Self-training with noisy student improves imagenet classification. *arXiv preprint arXiv:1911.04252*, 2019.
- [44] Sergey Zagoruyko and Nikos Komodakis. Wide residual networks. *arXiv preprint arXiv:1605.07146*, 2016.
- [45] Hongyi Zhang, Moustapha Cisse, Yann N Dauphin, and David Lopez-Paz. mixup: Beyond empirical risk minimization. *International Conference on Learning Representations (ICLR)*, 2018.

Supplementary Material:

Distribution Aligning Refinery of Pseudo-label for Imbalanced Semi-supervised Learning

A Proof of Theorem 1

In this section, we present the formal proof of Theorem 1. To this end, we interpret DARP as a coordinate ascent algorithm of the Lagrangian dual of its original objective (1), and discuss the necessary and sufficient condition of correct convergence of DARP, i.e., convergence to the optimal solution of (1).

More generally, we consider the following problem: For $A \in \mathbb{R}_{\geq 0}^{n \times m}$, $r \in \mathbb{R}_{\geq 0}^n$, $c \in \mathbb{R}_{\geq 0}^m$ and $w \in \mathbb{R}_{\geq 0}^m$ such that $\|r\|_1 = \|c\|_1$, find the solution M of the below convex optimization problem.

$$\begin{aligned} & \underset{M \in \mathbb{R}_{\geq 0}^{n \times m}}{\text{minimize}} && \sum_{i=1}^n \sum_{j=1}^m w_i M_{ij} \log \frac{M_{ij}}{A_{ij}} \\ & \text{subject to} && M \mathbf{1}_m = r \quad M^\top \mathbf{1}_n = c \end{aligned} \quad (3)$$

where $\mathbf{1}_n$ denotes the n -dimensional vector consisting of ones. We note that the above problem is well-known in information theory as the I-projection [11] when $w_i = 1 \ \forall i$. Now, we will show that DARP is indeed a coordinate ascent algorithm for the dual of the above optimization. To this end, we formulate the Lagrangian dual of (3).

Lemma 1. *The Lagrangian dual of (3) is given by*

$$\underset{\lambda \in \mathbb{R}^n, \nu \in \mathbb{R}^m}{\text{maximize}} \quad g(\lambda, \nu) = - \sum_{i=1}^n \sum_{j=1}^m w_i A_{ij} e^{-\frac{w_i + \lambda_i + \nu_j}{w_i}} - \sum_{i=1}^n \lambda_i r_i - \sum_{j=1}^m \nu_j c_j \quad (4)$$

In addition, the optimal objective value of (3) is equivalent to that of (4), i.e., the strong duality holds. Here, the primal optimal solution M of (3) and the dual optimal solutions λ, ν of (4) satisfies that

$$M_{ij} = A_{ij} e^{-\frac{w_i + \lambda_i + \nu_j}{w_i}} \quad \forall i, j \quad (5)$$

We provide the formal proof of Lemma 1 in Section B.1 for the completeness. Apparently, (4) is a concave optimization problem and solving (4) directly provides the optimal solution of (3) due to the last statement of Lemma 1. To show the connection between DARP and (4), we introduce the below lemma. We present the formal proof of the below lemma in Section B.2.

Lemma 2. *A pair (λ, ν) is the unique optimal solution of (4) if and only if the below equalities hold:*

$$\sum_{j=1}^m A_{ij} e^{-\frac{w_i + \lambda_i + \nu_j}{w_i}} = r_i, \quad \sum_{i=1}^n A_{ij} e^{-\frac{w_i + \lambda_i + \nu_j}{w_i}} = c_j. \quad (6)$$

In addition, for the coordinate ascent updates x^*, y^* for (4) defined by

$$\lambda^* := \underset{\lambda \in \mathbb{R}_{\geq 0}^n}{\text{argmax}} g(\lambda, \nu), \quad \nu^* := \underset{\nu \in \mathbb{R}_{\geq 0}^m}{\text{argmax}} g(\lambda, \nu). \quad (7)$$

find the solutions of the former and latter equality of (6), respectively.

By substituting $X_i = e^{-\frac{\lambda_i + w_i}{w_i}}$, $Y_j = e^{-\nu_j}$, one can verify that DARP is exactly a coordinate ascent (7). Therefore, we conclude that DARP indeed optimizes the dual of (3) and it finds the unique optimum M once it converges due to the last statement of Lemma 1. In particular, its correct convergence is guaranteed if the unique critical point of $g(\lambda, \nu)$ exists, i.e., there exists λ, ν satisfying (6).

B Proofs of technical Lemmas

B.1 Proof of Lemma 1

The Lagrangian dual function $g(\lambda, \nu)$ is defined by

$$g(\lambda, \nu) := \inf_{M \in \mathbb{R}_{\geq 0}^{n \times m}} \sum_{i=1}^n \sum_{j=1}^m w_i M_{ij} \log \frac{M_{ij}}{A_{ij}} + \sum_{i=1}^n \lambda_i \left(\sum_{j=1}^m M_{ij} - r_i \right) + \sum_{j=1}^m \nu_j \left(\sum_{i=1}^n M_{ij} - c_j \right). \quad (8)$$

Since g is convex with respect to M , the desired M can be computed by finding the critical point, i.e., M minimizes the above objective if and only if each M_{ij} satisfies

$$w_i \log \frac{M_{ij}}{A_{ij}} + w_i + \lambda_i + \nu_j = 0 \quad \Leftrightarrow \quad M_{ij} = A_{ij} e^{-\frac{w_i + \lambda_i + \nu_j}{w_i}}. \quad (9)$$

Using the above identity, we reformulate (8) as

$$\begin{aligned} g(\lambda, \nu) &= \sum_{i=1}^n \sum_{j=1}^m w_i A_{ij} e^{-\frac{w_i + \lambda_i + \nu_j}{w_i}} \left(-\frac{w_i + \lambda_i + \nu_j}{w_i} \right) \\ &\quad + \sum_{i=1}^n \lambda_i \left(\sum_{j=1}^m A_{ij} e^{-\frac{w_i + \lambda_i + \nu_j}{w_i}} - r_i \right) + \sum_{j=1}^m \nu_j \left(\sum_{i=1}^n A_{ij} e^{-\frac{w_i + \lambda_i + \nu_j}{w_i}} - c_j \right) \\ &= - \sum_{i=1}^n \sum_{j=1}^m w_i A_{ij} e^{-\frac{w_i + \lambda_i + \nu_j}{w_i}} - \sum_{i=1}^n \lambda_i r_i - \sum_{j=1}^m \nu_j c_j \end{aligned} \quad (10)$$

Hence, the Lagrangian dual of (3) is given by (4). Since the optimization (3) satisfies the Slater's condition, i.e., there exists a feasible solution of (3) [36, 6], the strong duality holds. Finally, the optimal solution M of (3) satisfies $M_{ij} = A_{ij} e^{-\frac{w_i + \lambda_i + \nu_j}{w_i}}$ due to (9). This completes the proof of Lemma 1

B.2 Proof of Lemma 2

It is straightforward to derive that

$$\frac{g(\lambda, \nu)}{\partial \lambda_i} = \sum_{j=1}^m A_{ij} e^{-\frac{w_i + \lambda_i + \nu_j}{w_i}} - r_i, \quad \frac{g(\lambda, \nu)}{\partial \nu_j} = \sum_{i=1}^n A_{ij} e^{-\frac{w_i + \lambda_i + \nu_j}{w_i}} - c_j.$$

Since $g(\lambda, \nu)$ is concave for λ (or ν) given ν (or λ), λ^* (or ν^*) is a coordinate ascent update if and only if $\frac{g(\lambda, \nu)}{\partial \lambda} = \mathbf{0}_n$ (or $\frac{g(\lambda, \nu)}{\partial \nu} = \mathbf{0}_m$). This directly implies the second statement of Lemma 2 and completes the proof of Lemma 2.

C Experimental results on CIFAR-100 and STL-10

Table 4: Comparison of classification performance (bACC/GM) on CIFAR-100 and STL-10 under two different class-imbalance ratio γ_l . SSL denotes semi-supervised learning and RB denotes re-balancing. The numbers in brackets below the gray rows are relative test error gains from DARP, compared to applied baseline SSL algorithms, respectively. The best results are indicated in bold.

Algorithm	SSL	RB	CIFAR-100		STL-10	
			$\gamma_l = 10$	$\gamma_l = 20$	$\gamma_l = 10$	$\gamma_l = 20$
Vanilla	-	-	55.9 \pm 0.12 / 50.7 \pm 0.12	49.5 \pm 0.03 / 40.3 \pm 0.04	56.4 \pm 1.50 / 51.8 \pm 1.67	48.1 \pm 0.26 / 38.2 \pm 0.67
Re-sampling	-	✓	54.6 \pm 0.05 / 48.9 \pm 0.40	48.1 \pm 0.17 / 38.3 \pm 0.82	57.8 \pm 0.76 / 53.6 \pm 0.80	47.4 \pm 0.16 / 35.8 \pm 0.11
LDAM-DRW	-	✓	55.7 \pm 0.75 / 51.6 \pm 0.08	50.4 \pm 0.32 / 45.4 \pm 0.98	58.0 \pm 0.53 / 54.4 \pm 0.84	50.2 \pm 0.05 / 42.4 \pm 0.08
cRT	-	✓	56.2 \pm 0.36 / 52.2 \pm 0.38	50.7 \pm 0.11 / 43.8 \pm 0.04	59.2 \pm 0.53 / 55.7 \pm 0.65	49.2 \pm 0.29 / 42.3 \pm 0.20
VAT	✓	-	54.6 \pm 0.06 / 48.6 \pm 0.11	48.5 \pm 0.16 / 38.5 \pm 0.25	64.2 \pm 0.33 / 61.1 \pm 0.50	56.2 \pm 0.03 / 50.5 \pm 0.08
Mean-Teacher	✓	-	54.1 \pm 0.13 / 48.2 \pm 0.05	48.2 \pm 0.13 / 37.6 \pm 0.07	57.7 \pm 0.10 / 54.8 \pm 0.87	48.0 \pm 0.47 / 35.3 \pm 3.81
MixMatch	✓	-	60.1 \pm 0.39 / 48.1 \pm 0.48	53.4 \pm 0.04 / 41.9 \pm 0.16	56.3 \pm 0.46 / 48.2 \pm 1.08	45.2 \pm 0.19 / 22.0 \pm 0.12
MixMatch + DARP	✓	-	60.9 \pm 0.24 / 55.8 \pm 0.05	54.8 \pm 0.27 / 45.6 \pm 0.48	67.9 \pm 0.24 / 65.1 \pm 0.51	58.3 \pm 0.73 / 52.2 \pm 1.01
			(-2.04% / -14.8%)	(-3.38% / -6.33%)	(-26.7% / -32.7%)	(-23.9% / -38.8%)
ReMixMatch	✓	-	59.2 \pm 0.03 / 52.1 \pm 0.13	53.5 \pm 0.03 / 42.3 \pm 0.13	67.8 \pm 0.45 / 61.1 \pm 0.92	60.1 \pm 1.18 / 44.9 \pm 1.52
ReMixMatch + DARP	✓	-	59.8 \pm 0.20 / 52.9 \pm 0.41	54.4 \pm 0.07 / 44.2 \pm 0.07	79.4 \pm 0.07 / 78.2 \pm 0.10	70.9 \pm 0.44 / 67.0 \pm 1.62
			(-1.25% / -1.59%)	(-1.88% / -3.23%)	(-36.0% / -44.0%)	(-27.0% / -40.0%)
FixMatch	✓	-	60.1 \pm 0.05 / 54.4 \pm 0.11	54.0 \pm 0.04 / 44.4 \pm 0.17	72.9 \pm 0.09 / 69.6 \pm 0.01	63.4 \pm 0.21 / 52.6 \pm 0.09
FixMatch + DARP	✓	-	61.1 \pm 0.23 / 56.4 \pm 0.28	54.9 \pm 0.05 / 46.4 \pm 0.41	77.8 \pm 0.33 / 76.5 \pm 0.40	69.9 \pm 1.77 / 65.4 \pm 3.07
			(-2.55% / -4.40%)	(-1.97% / -3.60%)	(-18.2% / -22.8%)	(-17.9% / -27.0%)

In this section, we present additional experimental results on CIFAR-100 [25] and STL-10 [10] datasets. In the case of CIFAR-100, we construct its “synthetically long-tailed” variant with $N_l = 300$, $M_l = 150$ as done in Section 4.1. Here, we assume that labeled and unlabeled datasets have the same class distribution, i.e., $\gamma_l = \gamma_u$. Since STL-10 is originally composed of a balanced labeled dataset with $N_k = 500$ for $k = 1, \dots, 10$, we construct “synthetically long-tailed” variant with $N_l = 450$ for a labeled dataset. As an unlabeled dataset, we fully use a given unlabeled dataset in STL-10 with $M = 100,000$, whose class distribution is unknown. Hence, in case of STL-10, we use the estimated distribution $\{M_k\}_{k=1}^K$ for DARP as previously conducted in Table 2. Table 4 summarizes the performance of baseline algorithms and DARP for learning both CIFAR-100 and STL-10. One can verify that DARP consistently improves the applied SSL algorithms for both datasets. It is also noticeable that the gain from DARP is significant on STL-10. This is because the mismatch of labeled and unlabeled datasets is significant in STL-10 since the given unlabeled dataset is usually assumed to be closed to the uniform distribution [10, 5]. Consequently, this result shows the importance of consideration of distribution mismatch between labeled and unlabeled data again, and the superiority of DARP for resolving this.

D Experimental results on SUN397

Table 5: Comparison of classification performance (bACC/GM) on SUN397. SSL denotes semi-supervised learning and RB denotes re-balancing. The numbers in brackets below the gray rows are relative test error gains from DARP, compared to applied baseline SSL algorithms, respectively. The best results are indicated in bold.

Method	SSL	RB	$\gamma \approx 46$
Vanilla	-	-	38.3 \pm 0.05 / 29.9 \pm 0.08
cRT	-	✓	39.3 \pm 0.21 / 33.7 \pm 0.37
FixMatch	✓	-	44.9 \pm 0.11 / 35.7 \pm 0.66
FixMatch + DARP	✓	-	45.5\pm0.32 / 37.5\pm0.04 (-1.09% / -2.80%)

In this section, we further verify the effectiveness of DARP on the real-world imbalanced dataset, SUN-397 [41]. SUN-397 is a dataset for a scene categorization and originally consists of 108,754 RGB images labeled with 397 classes. Since the dataset itself does not provide any separated split for testing, we first hold-out 50 samples per each class for testing. After that, we artificially construct the labeled and unlabeled dataset using the remaining dataset under $\frac{M_k}{N_k} = 2$. See Figure 3 for the class distribution of constructed dataset. With this dataset, we compare the models trained under 4 representative algorithms: vanilla, classifier re-training (cRT) [22], FixMatch [37] and FixMatch+DARP. Table 5 summarizes the experimental results. Here, DARP surpasses all the baseline algorithms, and this result shows the extensibility of DARP toward the real-world dataset.

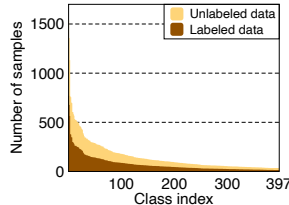


Figure 3: Class distribution of labeled and unlabeled dataset of SUN-397.

Training details. For pre-processing, we randomly crop and rescale to 224×224 size all labeled and unlabeled training images before applying augmentation. Following the experimental setups in [37], our batch contains 128 labeled data and 640 unlabeled data on each step. Here, we use standard ResNet-34 [18] model and train it for 300 epochs of unlabeled data using SGD optimizer with momentum 0.9. We utilize linear learning rate warmup for the first 5 epochs until it reaches an initial value of 0.4. Then, we decay the learning rate at epochs 60, 120, 160, and 200 epochs by dividing it by 10. For applying FixMatch [37], we use unlabeled loss weight $\lambda_u = 5$ and confidence threshold $\tau = 0.7$. We utilize Exponential moving average technique with decay 0.9 and use RandAugment with random magnitude [12] for strong augmentation and random horizontal flip for weak augmentation.

E Combination of re-balancing and semi-supervised learning

Table 6: Comparison of classification performance (bACC/GM) on CIFAR-10 under three different class-imbalance ratio $\gamma = \gamma_l = \gamma_u$. SSL denotes semi-supervised learning and RB denotes re-balancing. The numbers in brackets below the gray rows are relative test error gains from DARP, compared to applied baseline SSL algorithms, respectively. The best results are indicated in bold.

Algorithm			CIFAR-10		
	SSL	RB	$\gamma = 50$	$\gamma = 100$	$\gamma = 150$
Vanilla	-	-	65.2 \pm 0.05 / 61.1 \pm 0.09	58.8 \pm 0.13 / 51.0 \pm 0.11	55.6 \pm 0.43 / 44.0 \pm 0.98
ReMixMatch [4]	✓	-	81.5 \pm 0.26 / 80.2 \pm 0.32	73.8 \pm 0.38 / 69.5 \pm 0.84	69.9 \pm 0.47 / 62.5 \pm 0.35
ReMixMatch + DARP	✓	-	82.1 \pm 0.14 / 80.8 \pm 0.09 (-3.45% / -3.52%)	75.8 \pm 0.09 / 72.6 \pm 0.24 (-7.84% / -10.2%)	71.0 \pm 0.27 / 64.5 \pm 0.68 (-3.60% / -5.19%)
ReMixMatch + cRT	✓	✓	86.8 \pm 0.50 / 86.5 \pm 0.49	81.4 \pm 0.41 / 80.7 \pm 0.45	78.9 \pm 0.84 / 77.8 \pm 0.94
ReMixMatch + DARP + cRT	✓	✓	87.3\pm0.16 / 87.0\pm0.11 (-4.33% / -3.63%)	83.5\pm0.07 / 83.1\pm0.09 (-11.3% / -12.2%)	79.7\pm0.54 / 78.9\pm0.49 (-3.61% / -5.12%)

Meanwhile DARP outperforms all the baselines, it could be further improved by combining with RB algorithms. To verify this, we examine DARP and baseline SSL algorithm, ReMixMatch [4], by combining with the classifier re-training (cRT) algorithm [22], which is a recently introduced state-of-the-art RB algorithm. These algorithms are denoted by “ReMixMatch + cRT” and “ReMixMatch + DARP + cRT”, respectively, and the detailed implementation can be found in Section G. Table 6 summarizes the performance of ReMixMatch with/without DARP combined with cRT. One can observe that combining with cRT improves both ReMixMatch and DARP significantly, but DARP still outperforms ReMixMatch under cRT. For example, DARP exhibits 11.3%/12.2% relative error gains of bACC/GM compared to ReMixMatch when $\gamma = \gamma_l = \gamma_u = 100$.

F Estimation of class distribution of unlabeled dataset

Recall that DARP requires the true class distribution of unlabeled dataset, $\{M_k\}_{k=1}^K$, which is not known for the learner in general. Hence, we estimate it using the confusion matrix and it successfully works in Table 2. In this section, we present more details about this estimation. First, the confusion matrix of unlabeled dataset $C^{\text{unlabeled}} \in \mathbb{R}^{K \times K}$ is defined as follow:

$$C_{ij}^{\text{unlabeled}} := \frac{\sum_{m: y_m^{\text{unlabeled}}(j)=1} f_i(x_m^{\text{unlabeled}})}{|\{m \mid y_m^{\text{unlabeled}}(j) = 1\}|}$$

where it denotes the empirical probability that the model $f = [f_k]_{k=1}^K : \mathbb{R}^d \rightarrow [0, 1]^K$ predicting class i when the true class is j and $f_k(x) \in [0, 1]$ is the predictive probability for class k given an input x . Then, the confusion matrix $C^{\text{unlabeled}}$ has the following linear relationship with the model's prediction and the true number of data in each class:

$$\begin{bmatrix} \sum_{m=1}^M f_1(x_m^{\text{unlabeled}}) \\ \vdots \\ \sum_{m=1}^M f_K(x_m^{\text{unlabeled}}) \end{bmatrix} = C^{\text{unlabeled}} \times \begin{bmatrix} |\{m \mid y_m^{\text{unlabeled}}(1) = 1\}| \\ \vdots \\ |\{m \mid y_m^{\text{unlabeled}}(K) = 1\}| \end{bmatrix} = C^{\text{unlabeled}} \times \begin{bmatrix} M_1 \\ \vdots \\ M_K \end{bmatrix}$$

From the above equation, we can estimate class distribution $\{M_k\}_{k=1}^K$ as follow:

$$\begin{bmatrix} M_1 \\ \vdots \\ M_K \end{bmatrix} = (C^{\text{unlabeled}})^{-1} \times \begin{bmatrix} \sum_{m=1}^M f_1(x_m^{\text{unlabeled}}) \\ \vdots \\ \sum_{m=1}^M f_K(x_m^{\text{unlabeled}}) \end{bmatrix}$$

However, to obtain the confusion matrix $C^{\text{unlabeled}}$, the true labels for unlabeled dataset are required which do not exist. To circumvent this, we approximate it using the given labeled dataset $\mathcal{D}^{\text{labeled}}$. Namely, we split the labeled dataset $\mathcal{D}^{\text{labeled}} = \{(x_n^{\text{labeled}}, y_n^{\text{labeled}})\}_{n=1}^N$ into $\mathcal{D}^{\text{labeled}} = \mathcal{D}^{\text{est}} \cup \mathcal{D}^{\text{train}}$ where $\mathcal{D}^{\text{est}} \cap \mathcal{D}^{\text{train}} = \emptyset$. Then, we train another classifier $g : \mathbb{R}^d \rightarrow [0, 1]^K$ using $\mathcal{D}^{\text{train}}$, and obtain the confusion matrix C^{est} using g on \mathcal{D}^{est} . For our experiments, we construct \mathcal{D}^{est} by taking 10 samples for each class and train a classifier g using a vanilla scheme. After that, we train a classifier f by fully utilizing $\mathcal{D}^{\text{labeled}}$ for a training dataset with C^{est} as the estimation of $C^{\text{unlabeled}}$. This estimation assumes that two confusion matrices of labeled and unlabeled datasets are similar. It is true when both labeled and unlabeled datasets are constructed from the same distribution as we have assumed so far. Also, it is worth noting that similar approaches are used in the case of noisy labels [19] and domain adaptation [3].

G Implementation details

All experiments are conducted with Wide ResNet-28-2 [31] and it is trained with batch size 64 for 2.5×10^5 training iterations except Section D. For training with semi-supervised learning algorithms, we use Adam optimizer [24] with a learning rate 2×10^{-3} . For the hyperparameters of Adam, we use $\beta_1 = 0.9$, $\beta_2 = 0.999$ and $\varepsilon = 10^{-8}$ which is a default choice of [24]. To evaluate models trained by semi-supervised learning algorithms, we use an exponential moving average of its parameters with a decay rate 0.999 and apply weight decay of 4×10^{-4} at each update following [5].⁴ For training with re-balancing algorithms, we use SGD with a learning rate 0.1, momentum 0.9 and weight decay 5×10^{-4} . The learning rate of SGD decays by 0.01 at the time step 80% and 90% of the total iterations following [8]. For all algorithms, we evaluate the model on the test dataset for each 500 iterations and report the average test accuracy of the last 20 evaluations following [5].

DARP. We apply DARP procedure for each 10 iterations with fixed hyper-parameters $\alpha = 2$ and $T = 10$, which is empirically enough for the convergence of DARP. To show its convergence empirically, we directly measure the distribution mismatch as $\frac{1}{M} \sum_{k=1}^K |\tilde{M}_k - M_k|$ for each iteration, where \tilde{M}_k implies the resulting class distribution of refined pseudo-labels. For additional comparison, we also report the results from distribution alignment (DA) term of ReMixMatch [4]. We use the model trained using MixMatch [5] under 3 cases: (1) $\gamma_l = 100, \gamma_u = 1$, (2) $\gamma = \gamma_l = \gamma_u = 100$ (reverse) and (3) $\gamma = 100$. Figure 4 shows that $T = 10$ is enough for the convergence and DARP’s superiority compared to DA. The effect of α is presented in Section 4.3. Since the estimation is not accurate at the early stage of training, we are not using DARP until the first 40% of iterations.

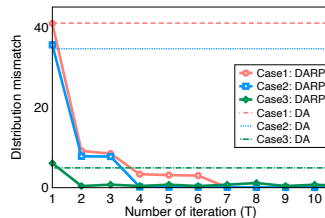


Figure 4: Distribution matching via DARP for each iteration.

VAT, Mean-Teacher and MixMatch. In the experiments, we use VAT [30], Mean-Teacher [38] and MixMatch [5] as the baselines for semi-supervised learning methods. Since these methods have some hyperparameters, we use the same values for them as used in [5]. For VAT, the consistency coefficient λ_u is set to 0.3, the norm constraint for adversarial perturbation ϵ is set to 1.0 and the norm of initial perturbation ζ is set to 1.0×10^{-6} . For Mean-Teacher, the consistency coefficient λ_u is set to 50 and the EMA model used for the evaluation is reused for the consistency regularization. Following [38], we ramped up the consistency coefficient starting from 0 to λ_u using a sigmoid schedule so that it achieves the maximum value at 1.0×10^5 iterations for both methods. For MixMatch, we set temperature T as 0.5, the number of augmentation K as 2, the parameter for beta distribution α as 0.75 and the consistency coefficient λ_u as 75. During the entire iterations, the consistency coefficient is linearly increased to λ_u started from 0.

ReMixMatch. For ReMixMatch [4], we use $K = 2$ for the number of augmentations to balance the improvement from an augmentation anchoring and a computational cost. Also, we use RandAugment [12] as a strong augmentation which is shown to be substitutable with CTAugment [37]. For the other hyperparameters, we use the same values used in the original paper.

FixMatch. For FixMatch [37], we use $\mu = 2$ for the ratio of unlabeled data μ and Adam optimizer as described in Section 4.1 to fairly compare it with ReMixMatch. For the other hyperparameters, λ_u used for balancing the loss from labeled and unlabeled data and τ used as a threshold for pseudo-labeling [27], we use the same values with the original paper, $\lambda_u = 1$ and $\tau = 0.95$.

cRT. To re-balance the network trained under the imbalanced class distribution, we use the classifier re-training (cRT) scheme [22]. After training the network regardless of the use of unlabeled data without considering the imbalance, we re-initialize the linear classifier of the network and only re-train it for 1.0×10^4 iterations by freezing other parameters. We re-balance the training objective by re-weighting the given loss [23] instead of re-sampling. Also, we re-train the classifier using only the labeled dataset.

⁴We do not use the exponential moving average for evaluating “re-balancing” algorithms as it hurts the performance.